INTEGRIN BETA-1 RECRUITMENT AT CELL-MATRIX ADHESIONS IN AGED VASCULAR SMOOTH MUSCLE CELLS

An Undergraduate Research Scholars Thesis

by

FRIDA LEON OLMEDO

Submitted to the LAUNCH: Undergraduate Research office at
Texas A&M University
in partial fulfillment of requirements for the designation as an

UNDERGRADUATE RESEARCH SCHOLAR

Approved by
Faculty Research Advisor: Andreea Trache, Ph.D.

May 2021

Major: Biomedical Engineering

RESEARCH COMPLIANCE CERTIFICATION

Research activities involving the use of human subjects, vertebrate animals, and/or biohazards must be reviewed and approved by the appropriate Texas A&M University regulatory research committee (i.e., IRB, IACUC, IBC) before the activity can commence. This requirement applies to activities conducted at Texas A&M and to activities conducted at non-Texas A&M facilities or institutions. In both cases, students are responsible for working with the relevant Texas A&M research compliance program to ensure and document that all Texas A&M compliance obligations are met before the study begins.

I, Frida Leon Olmedo, certify that all research compliance requirements related to this Undergraduate Research Scholars thesis have been addressed with my Research Faculty Advisor prior to the collection of any data used in this final thesis submission.

This project required approval from the Texas A&M University Research Compliance & Biosafety office.

Institutional Biosafety Committee

Before initiating this study, approval was received from the Texas A&M University Institutional Biosafety Committee (IBC 2019-100). Expiration date: 10/24/2022.

Vertebrate Animals

Before initiating this study, approval was received from the Texas A&M University Institutional Animal Care and Use Committee (AUP 2019-0033). Fischer 344 rats were obtained from the National Institute on Aging and housed at the Texas A&M Comparative Medicine Program Facility.

TABLE OF CONTENTS

ABSTRACT

Integrin Beta-1 Recruitment at Cell-matrix Adhesions in Aged Vascular Smooth Muscle Cells

Frida Leon Olmedo
Department of Biomedical Engineering
Texas A&M University

Research Faculty Advisor: Andreea Trache, Ph.D.
Department of Medical Physiology Texas A&M University Health Science Center
Department of Biomedical Engineering
Texas A&M University

Arterial aging is characterized by reduced vessel contractility, arterial stiffening and endothelial dysfunction which are major predictors of cardiovascular diseases present in the elder population. At the level of vascular smooth muscle cells, this corresponds to age-induced phenotypic changes from a contractile to a synthetic phenotype associated with decreased mechanosensitive responses to external stimuli in these cells. This study is focused on analyzing the integrin role as a contributor to arterial vasomotor dysfunction through the regulation of vascular smooth muscle cells adhesion to extracellular matrix components. To test the effects of matrix-functionalized substrate stiffness on integrin spatial distribution, vascular smooth muscle cells isolated from soleus feed arteries of young and old Fisher 344 rats were plated on glass-bottom cell culture dishes functionalized with matrix proteins, fibronectin and collagen I. Then, cells were stained for endogenous beta-1 integrin using mouse anti-beta-1-Alexa 488 direct-labeled antibody (Biolegend, San Diego, CA). Stained cells were imaged using total internal reflection fluorescence and confocal microscopy to analyze spatial distribution of

beta-1 integrin at cell-matrix adhesions. Our results showed a significantly higher fluorescence intensity, indicating a greater amount of integrin beta-1 present at cell-matrix adhesions in young versus old vascular smooth muscle cells, in all conditions. The decrease of beta-1 integrin recruitment at cell-matrix adhesions in old cells, shows a reduced cell adhesion to the matrix that correlates well with the decreased contractility of aged vascular smooth muscle cells.

The work presented here, partially references the abstract accepted to the 65th Biophysical Society Meeting (Ojha et al 2021).

DEDICATION

To my family, my friends and Dr. Andreea Trache, who have believed in my potential, supported me throughout this research process and inspired me to achieve even more.

ACKNOWLEDGEMENTS

Contributors

I would like to thank my Research Faculty Advisor, Dr. Andreea Trache, and my fellow lab members, Dr. Krishna Ojha and Samuel Padgham, for their guidance and support throughout the course of this research.

Thanks also go to my professors and the department staff for making my time at Texas A&M University a great experience.

Finally, thanks to all my friends for their encouragement and to my parents, Arturo Leon Romo and Georgina Olmedo Gonzalez, for their unconditional love.

The data used for "INTEGRIN BETA-1 RECRUITMENT AT CELL-MATRIX ADHESION IN AGED VASCULAR SMOOTH MUSCLE CELLS" were provided by my Research Faculty Advisor, Dr. Andreea Trache. The analyses presented in "INTEGRIN BETA-1 RECRUITMENT AT CELL-MATRIX ADHESION IN AGED VASCULAR SMOOTH MUSCLE CELLS" were conducted by me, Frida Leon Olmedo. These data are currently unpublished; however, they will be submitted to a peer-review journal, Summer 2021.

All other work conducted for the thesis was completed by Frida Leon Olmedo independently.

Funding Sources

This undergraduate research work was made possible in part by the NIA, under Grant No. 1-R03-AG-064551-01 to Dr. Andreea Trache. Its contents are solely the responsibility of the authors and do not necessarily represent the official views of the NIA.

NOMENCLATURE

α	Alpha
$\alpha 1$	Alpha-1
$\alpha 2$	Alpha-2
$\alpha 5$	Alpha-5
$\alpha 1 \beta 1$	Alpha-1-beta-1
$\alpha 2 \beta 2$	Alpha-2-beta-2
$\alpha 5 \beta 1$	Alpha-5-beta-1
β	Beta
$\beta 1$	Beta-1
CO_2	Carbon Dioxide
Coll-I	Collagen-I
CVDs	Cardiovascular Diseases
DPBS	Dulbecco's Phosphate Buffered Saline
ECM	Extracellular Matrix
FA	Focal Adhesions
FN	Fibronectin
μL	Microliter
μm	Micrometer
mL	Milliliter
mm	Millimeter
ms	Millisecond

nm	Nanometer
N_2	Nitrogen
PFA	Paraformaldehyde
PMT	Photomultiplier tube
TC	Tissue culture
TIRF	Total Internal Reflection Fluorescence
Trypsin	Trypsin-EDTA
VSMC	Vascular Smooth Muscle Cells

1. INTRODUCTION

The growing prevalence of cardiovascular diseases (CVDs) is a pressing issue faced today. In a report submitted by the American Heart Association, in 2019 CVDs were the leading cause of death globally, accounting for more than 18.6 million deaths (Virani et al., 2021). Moreover, the cost of treating these diseases has an estimated expense of $351.3 billion (from 2014 to 2015) in the U.S. alone. Also, it is predicted that by 2035 there will be a sharp increase in the total expenses for patients 65 years or older (Virani et al. 2020).

Aging is a major risk factor for CVDs (Najjar et al., 2005), along with smoking, physical inactivity, and nutrition deficiencies (Virani et al., 2020). Previous research has shown that arterial aging is characterized by reduced vessel contractility, arterial stiffening, and endothelial dysfunction, all of which are considered major precursors of CVDs affecting the growing aging population (Donato et al., 2018). These age-induced vascular changes are incurred by a phenotypic change of vascular smooth muscle cells (VSMC), from a contractile to a synthetic phenotype which results in a decrease of cellular mechanosensitive responses to external stimuli (Trache et al., 2020). To understand how aging induces VSMC adaptation and simultaneous physiological changes in blood vessels, a brief introduction of cellular components and their microenvironment will follow.

The extracellular matrix (ECM) is an intricate network of macromolecules, including proteins, proteoglycans and regulatory factors that provide structural and biochemical support to the surrounding cells (Yue, 2014). Structural and/or compositional changes within the ECM affect cell response through the use of integrins. Integrins are transmembrane receptors that bind the cytoskeleton of the cells to the ECM via adhesion proteins at cell-matrix adhesion sites,

namely focal adhesions (FA). These heterodimeric glycoproteins are composed of two subunits: alpha (α) and beta (β). Each of the subunits has an extracellular domain that forms the ligand adhesion sites for extracellular proteins (Arnaout et al., 2007). Intracellularly, the β-tail of the integrin interacts with adhesion proteins at FA (Legate et al., 2009).

FA form intracellularly at sites of cell-matrix adhesion upon recruitment of specific signaling molecules (Zaidel-Bar et al. 2007; Martin et al. 2002; Davis et al. 2001). As a result, these are dynamic structures that undergo continual changes to facilitate cellular adaptation to mechanical stresses (Worth et al. 2001; Opazo Saez et al. 2004; Zamir & Geiger, 2001). FA also act as signaling centers for intracellular pathways that regulate cell growth, contractility and gene expression (Geiger et al., 2001). Due to their strategic location at the plasma membrane, integrins function as the main mediators of the cell-matrix crosstalk, regulating cell adhesion to ECM and signal transduction to the cellular cytoskeleton, ultimately inducing alterations of stress fiber formation via actin dynamics in response to external stimuli (Lakatta, 2003; Saphirstein et al., 2013).

The diagram in **Figure 1.1** shows distinct integrin subunits that are suitable receptors for collagen and fibronectin (FN). Due to the versatility of integrin $\beta1$ as a receptor for both ECM proteins, attributed to the different α complementary subunits, $\beta1$ can pair with $\alpha5$ to form integrin $\alpha5\beta1$ which is the main receptor for FN, and can also pair with $\alpha1$ or $\alpha2$ forming integrin $\alpha1\beta1$ or $\alpha2\beta2$, both of which are main receptors for collagen. Collagen I (Coll-I) is a major protein found in the ECM. It is known that collagen deposition increases with age (Trache et al., 2020; Zhang et al., 2016) and thus contributes to age-induced vessel wall stiffening. On the other hand, FN is a key protein used for mediating cell-matrix attachment. Both of these proteins

have distinct amino acid sequences that are recognized by specific integrin receptors (Takada et al., 2007).

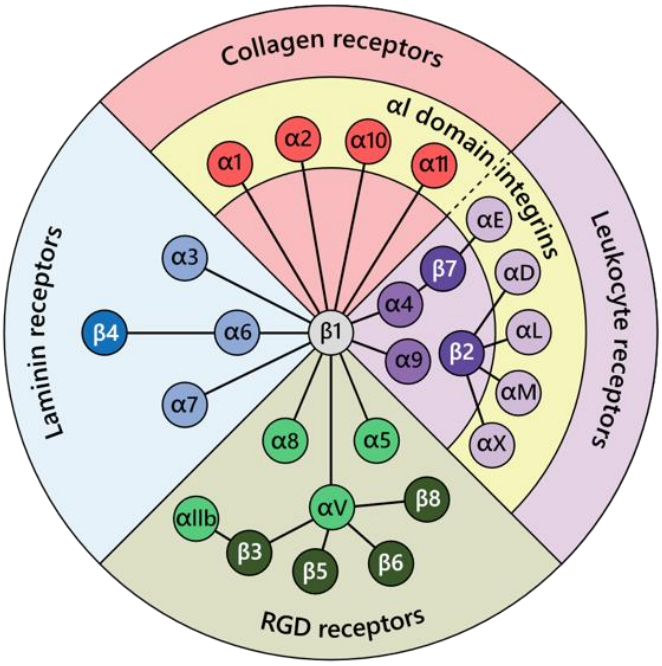

Figure 1.1: Diagram of known integrins and the specific extracellular matrices these recognize. Note that tripeptide Arg-Gly-Asp (RGD) is the amino acid sequence found in fibronectin. Figure adapted from (Morphic Therapeutic, 2018).

Supporting research has established a correlation between aging and the decrease of arterial vasoconstrictor responses (Delp et al., 1995; Kenney & Armstrong, 1996; Dinenno et al., 2002; Qiu et al., 2010). Additionally, several physiological functions of arteries such as regulating blood pressure, blood flow and vessel resistance are modulated by the intrinsic ability of VSMC adaptation to mechanical stimuli (Janmey & McCulloch, 2007; Janmey et al., 2009; Luo et al., 2008; Martinez-Lemus et al., 2003).

This study aims to understand the age-induced effects on VSMC morphological adaptation to compositional changes in their microenvironment. Specifically, this research focuses on quantifying the $\beta 1$ integrin recruitment at FA for cells plated on glass dishes

functionalized with Coll-I and FN. Total internal reflection fluorescence and confocal microscopy were the selected imaging modalities for obtaining fluorescence images needed to quantify protein fluorescence at FA and through the entire cytoplasm of VSMC. Both of these techniques utilize minimal light exposure which mitigates the risk of cellular photo-toxicity (Lim et al., 2010). Fluorescence images obtained from TIRF and confocal microscopy were further analyzed using SlideBook software (Intelligent Imaging Innovations, Denver, CO, United States), followed by statistical analysis.

2. METHODS

The following sections describe the procedures used in this study to analyze the integrin-recruitment at focal adhesions in VSMC plated on ECM functionalized substrates.

2.1 Cell Culture

The cell culture of previously isolated VSMC from soleus feed arteries of young (4 months) and old (24 months) Fischer 344 rats is outlined in detail in the subsequent sections.

2.1.1 Vascular Smooth Muscle Cells Thawing

Frozen VSMC were removed from liquid nitrogen (N_2) and thawed in a 37°C water bath. The thawed cells were then transferred from their vial to a 15 mL Falcon tube, via a 10 mL pipet, containing 6 mL of warm (37°C) VSMC media. An additional 1 mL of media was used to wash the vial, which was then transferred to the cell suspension in the Falcon tube. The cell suspension was centrifuged using Eppendorf 5702 centrifuge set at 100 x g for 5 min. The supernatant, representing the remaining liquid above the solid cell pellet after centrifugation, was aspirated with a 10 mL pipet, while the pellet was gently re-suspended by adding 2 mL of warm VSMC media. This cell suspension was transferred to a 60 mm tissue culture (TC) dish, and an additional 2 mL of media were added to the dish. The cells were incubated overnight at 37°C with 5% CO_2.

2.1.2 Cell Expansion

After incubating overnight, the cells were examined using an Olympus CKX31 microscope using a 10X objective to ensure proper morphology and good cell attachment. Using sterile 5 mL pipets, the old media was replaced with fresh warm media, and VSMC were

incubated overnight. On the following day, the cells were examined for a confluence of at least 80% prior to expansion.

For the second step in cell culture expansion, the media was aspirated from the cells, which were then washed twice with 4 mL of sterile Dulbecco's Phosphate Buffered Saline (DPBS). The cells were treated with 0.4 mL of 0.25% trypsin-EDTA (trypsin) and placed in the incubator at 37°C for 1 min. Then, cells were mechanically detached by firmly tapping the dish; cell detachment was quickly checked under a microscope. Afterwards, the added trypsin was quenched with 2.6 mL of VSMC media. The cell suspension was transferred to a 100 mm dish, followed by the addition of 7 mL of media. The cells were incubated at 37°C with 5% CO_2.

A third step in the cell expansion process was performed by splitting the cells on a 1 to 3 ratio to facilitate the culture and expansion of VSMC for future experiments. First, the 100 mm dish containing the VSMC, was verified to be at least 80% confluent. A similar cell release procedure as above was followed, removing old media and washing the cells twice with DPBS, this time adding 0.6 mL of trypsin. Once cell detachment was verified using the microscope, 5.4 mL of VSMC media were pipetted into the dish to quench trypsin. Then, 2 mL of suspension were transferred into three 100 mm dishes, followed by the addition of 8 mL of fresh media to each. The cells were incubated at 37°C with 5% CO_2 and allowed to rest for a day.

2.1.3 Cell Harvesting

The next day, VSMC medium was removed, the cells were washed with 10 mL of DPBS twice, and 0.6 mL of trypsin were added to attain detachment of the cells from the dish. Immediately after, 2.4 mL of media were transferred to the cells. Lastly, the cell suspension was transferred to a sterile 15 mL Falcon tube, followed by the addition of 4 mL of VSMC media to the suspension, which was pipetted 5 times to obtain an even suspension.

2.1.4 Cell counting and Placing

This procedure is conducted right after cell harvesting, and it is useful in determining the amount of suspension needed in each of the designated dishes that will be used for an imaging experiment. For this protocol, we took a 10 μL sample and placed it into the hemocytometer using a micropipette. Then, the hemocytometer was placed on the Olympus CKX31 microscope, and using a 10X objective the cells were counted in all four corner grids, excluding the cells along the upper and left edges of those grids. **Figure 2.1** depicts the location of the cells that would be considered for cell counting (green circles) either within the corner grid and/or along the green outlines. On the other hand, the cells that would be discarded from cell counting are represented by red circles.

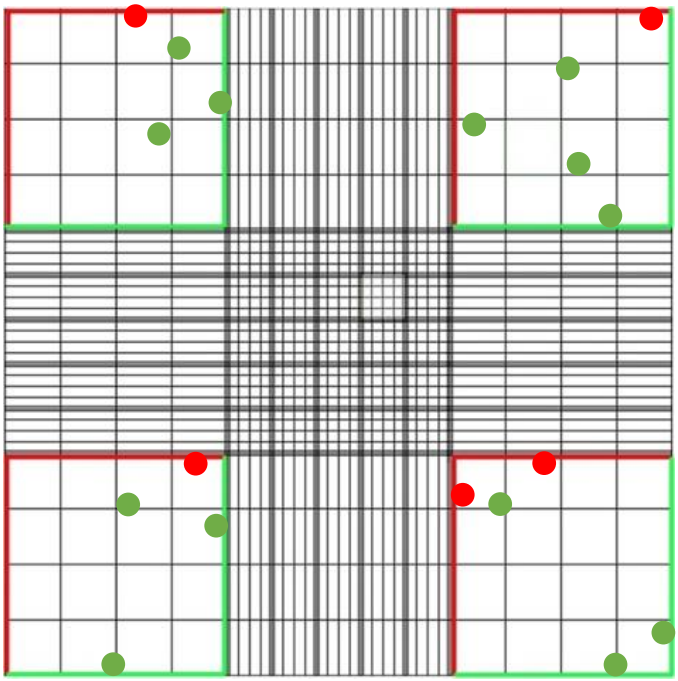

Figure 2.1: Hemocytometer grid for cell counting.

Following cell counting, the amount of suspension needed was calculated using the following equation, where N_c represents the number of cells counted on 4 grids of the

hemocytometer, V_s is the volume of suspension needed, and x is the quantity of cells needed for the experiment.

$$V_s = \frac{1}{\frac{N_C}{4} * 10{,}000} * x \ [\mu L] \quad . \qquad (2.1)$$

2.2 Immunofluorescence Staining

2.2.1 Cell Fixation

For imaging experiments, cells harvested and counted as above, were plated in 35 mm glass bottom dishes (MatTek, Ashland, MA). The following day, old media was removed, and the cells were washed twice with 37°C DPBS, followed by pipetting 1 mL of 2% paraformaldehyde (PFA) inside the fume hood and leaving the solution undisturbed for 10 min to fix the cells in culture.

2.2.2 Quench Washing and Rinsing

The PFA solution was aspirated and discarded into an appropriate waste disposal container. Then, 1 mL of cold glycine buffer was immediately added and left undisturbed for 5 min. This procedure was repeated two times, disposing of the buffer into an appropriate waste container afterwards. Lastly, the dish was rinsed once with 1 mL of DPBS to eliminate any excess PFA.

2.2.3 Antibody Labeling

In this research, VSMC were stained for endogenous $\beta 1$ integrin using anti-$\beta 1$-Alexa 488 direct-labeled antibody (BioLegend, San Diego, CA). Since the antibody used was pre-conjugated with its respective fluorophore, a regular 2-day procedure was reduced to one day preparation time. Thus, $1\mu L$ of primary antibody was mixed into 1mL of anti-body buffer, and subsequently added to the 35 mm dishes. Dishes were sealed with parafilm and incubated overnight at 4°C away from light. The following day, the dish was retrieved, and cells were

washed with 4°C antibody buffer 6 times, allowing for 5 min incubation intervals in between washes, followed by pipetting 1 mL of DPBS into each dish. Lastly, they were stored at 4°C until the imaging experiment was performed.

2.3 Imaging Techniques

Specific proteins can be detected through the use of fluorescence microscopy. Briefly, fluorescence microscopy utilizes light wavelengths to illuminate fluorophores coupled with antibodies. Antibodies are designed to recognize unique proteins. Fluorophores absorb light at a lower wavelength, emit light at a higher wavelength and are perceived as a color-specific glow against dark backgrounds when observed in an epifluorescence microscope, i.e., high fluorescence contrast against a dark background (Alberts et al., 1994). Two types of microscopy were used in this study to observe protein fluorescence distribution throughout VSMC.

2.3.1 Total Internal Reflection Fluorescence microscopy

Total Internal Reflection Fluorescence (TIRF) microscopy was used for fluorescence imaging and quantification at FA. This imaging technique uses the excitation of fluorophores present within approximately 90 nm of the plasma membrane (Seawright et al., 2018) in the immediate vicinity of the cell-coverslip interface (Trache & Meininger, 2008). TIRF microscopy provides optical images with high fluorescence contrast as a result of the evanescent wave that forms when light passes from a high refractive medium (e.g. glass) to a low refractive medium (e.g. VSMC) (Trache & Meininger, 2008).

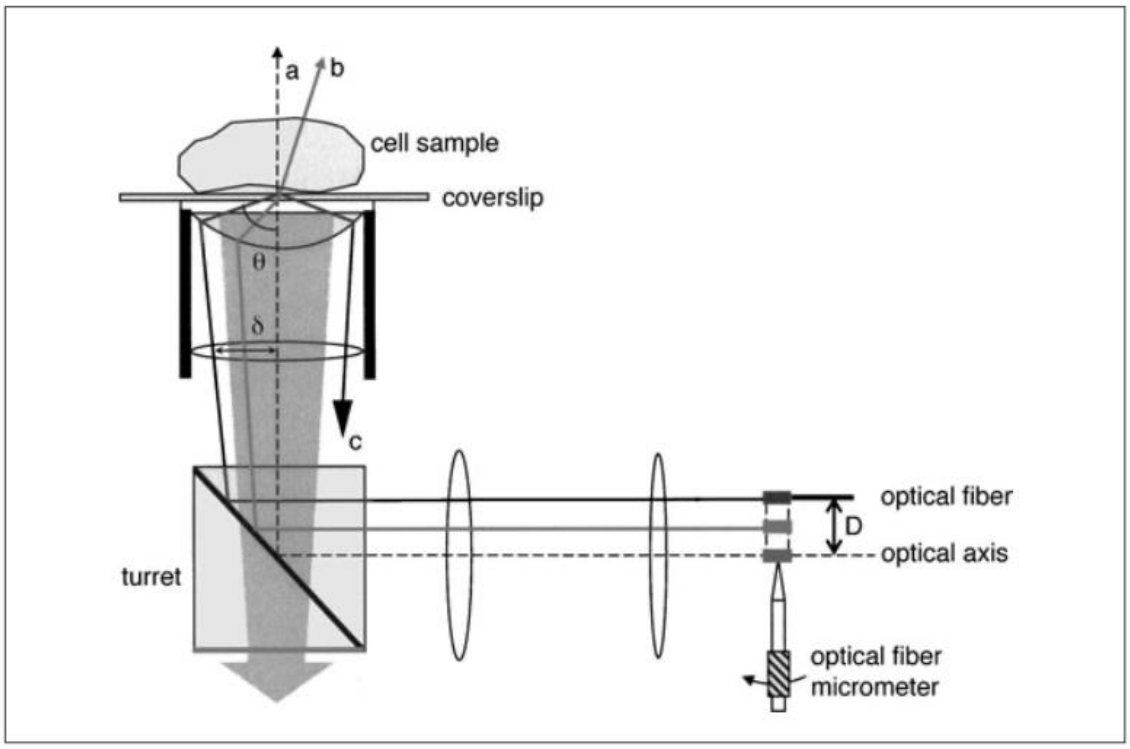

Figure 2.2: TIRF experimental setup and optical pathway. Figure adapted from Total Internal Fluorescence (TIRF) Microscopy (Trache & Meininger, 2008).

Figure 2.2 presents the optical path of the TIRF microscope. The micrometer located on the TIRF illuminator complex, permits movement of the optical fiber with respect to the optical axis (D). These distinct alignment configurations result in specific beam pathways. For instance, ray *a* is obtained by centering the optic fiber with the axis fiber, whereas ray *b* results from using an incident angle smaller than the critical angle in refence to the sample plane. Briefly, the incident angle dictates the incline of the incoming light, while the critical angle represents the maximum angle before a ray is completely reflected in a medium (Trache & Meininger, 2008). Thus, when the angle of incidence (θ) is greater than the critical angle, the refracted ray will not pass through the medium, but rather reflect back into it. This phenomenon is described as total internal reflection, represented by ray *c* (Trache & Meininger, 2008).

TIRF microscopy allows us to observe the fluorescence footprint of the cell plated on the glass bottom dishes; in a sense, the obtained images represent only the fluorescence of the proteins in the immediate vicinity of the plasma membrane 90 nm deep into the cell.

2.3.2 Confocal microscopy

Confocal microscopy is the imaging technique used for obtaining 3D optical scans to evaluate the entire fluorescence in the cell volume. The fluorescence images were collected using Fluoview 3000 confocal microscope (Olympus America, Inc., Waltham, MA) in stacks of 15 planes, with a step size of 0.25 μm and an exposure time of 100 ms, which were later used to create maximum projections for further analysis. This method was used for the observation and quantification of integrins throughout the cellular cytoplasm.

To achieve confocal imaging, excitation light from a laser is directed towards the sample (i.e. adherent cell in culture). The beam of light passes through a scanning system and reaches the objective, which focuses the scanning beam as a spot on the sample. Fluorescence emission generated by the sample scatters in all directions. Fluorescence from the focal plane of the sample returned via the objective and scanning system, is then reflected off the dichroic mirror and subsequently focused on the detector. In front of the detector is a spatial filter (pinhole) which defines the image of the light in the focal plane of the microscope. Most fluorescence originating from above or below the plane of focus of the sample is rejected by the pinhole, such that no out-of-focus light reaches the detector. The light collected from a single focal plane is called optical section (slice). The pinhole acts as a spatial filter allowing confocal light to reach the detector and to suppress light from non-focal planes. To form a 2D image plane, the laser beam scans the specimen in a raster pattern, that is, horizontally and vertically, then the fluorescence light is detected by a low-noise photomultiplier tube (PMT) and converted for

display on a computer screen (Hibbs 2004). The diagram depicted on **Figure 2.3** displays the light pathway and sample interaction of a confocal microscope.

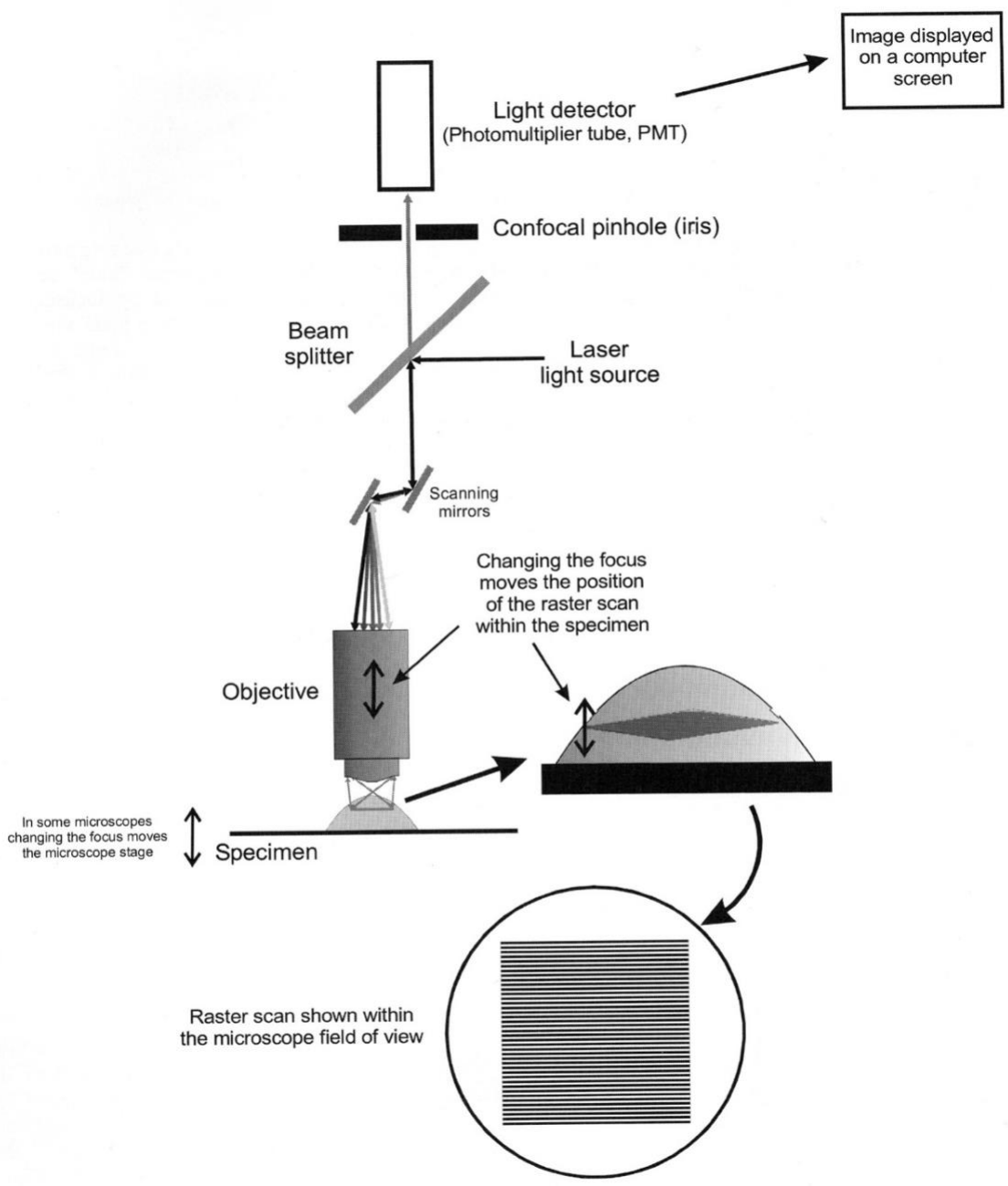

Figure 2.3: Confocal microscopy experimental setup and optical pathway. Figure from Confocal Microscopy for Biologists (Hibbs, 2004).

2.4 Image Analysis

2.4.1 Image Deconvolution and Background Subtraction

Using SlideBook 6.2 imaging software (Intelligent Imaging Innovations, Denver, CO), previously acquired images were imported into a new file. Fluorescence images are individually processed through a simple deconvolution which improves image contrast. Specifically, TIRF images use 'No Neighbors' algorithm given that each image represents a single fluorescence plane. On the other hand, confocal microscopy images are processed as a stack of fluorescence planes. Thus, 'Nearest Neighbors' algorithm is used to deblur the images by considering the planes adjacent (directly above and below) to the working plane, as main contributors to the out-of-focus blur. Additionally, to perform non-specific fluorescence background subtraction, a region of interest is selected to create a background mask. The mean intensity of this mask then serves as the offset value to create a new channel for the image, which will in turn minimize the noise of the original file, thus increasing signal-to-noise ratio. Both of these procedures are performed to obtain an image with higher contrast, allowing for a better characterization of the protein of interest; in this research, $\beta 1$ integrin fluorescence intensity.

2.4.2 Fluorescence Intensity Measurements

2.4.2.1 Fluorescence Intensity Analysis for TIRF Images

The segmenting procedure is used to obtain the protein ration of each imaged cell using TIRF microscopy. Following image deconvolution and background subtraction, a 'Segment' mask is placed on the image, which serves as a guiding point for adjusting the fluorescence intensity of the green channel, representative of integrin $\beta 1$ expression. The intensity threshold is modified so that it encompasses the FA. Upon obtaining the 'Segmenting' mask, the protein area is derived using mask statistics. Lastly, to standardize fluorescence readings so that they are

independent of cell size, a protein ratio of integrin $\beta 1$ is determined by diving the protein area by cell area for each cell. These values are recorded and subjected to further statistical analysis, using Student's t-test to create a comparison between young and old cells and the types of matrices used.

2.4.2.2 Fluorescence Intensity Analysis for Confocal Images

Once the images have been deconvolved and background subtracted, a 'Z-projection' is created from the stack of optical scans. Mean fluorescence readings are acquired for confocal images using a mask that outlines the cytoplasm of the cell. This mask then provides pre-determined statistical values including cell area, sum intensity and mean intensity. To statistically analyze a large number of cells, the mean fluorescence intensity values are calculated by dividing the sum fluorescence intensity by the cell area, for each cell. Similarly, these values are recorded and subjected to further statistical analysis to create a comparison between young and old cells using Student's t-test.

3. RESULTS

The following sections present the results obtained from the images collected using the previously described methods. A comparison between integrin β1 expression for cells plated on two different matrix proteins (FN and Coll-I), within young and old VSMC groups, will be presented in the subsequent sections.

3.1 Integrin β1 Morphology at Cell-Matrix Adhesions

Figure 3.1 shows TIRF representative fluorescence images for integrin β1 in young and old VSMC plated on FN and Coll-I matrix proteins. As previously described, TIRF microscopy reveals the cellular footprint of integrin β1 at the cell-substrate interface.

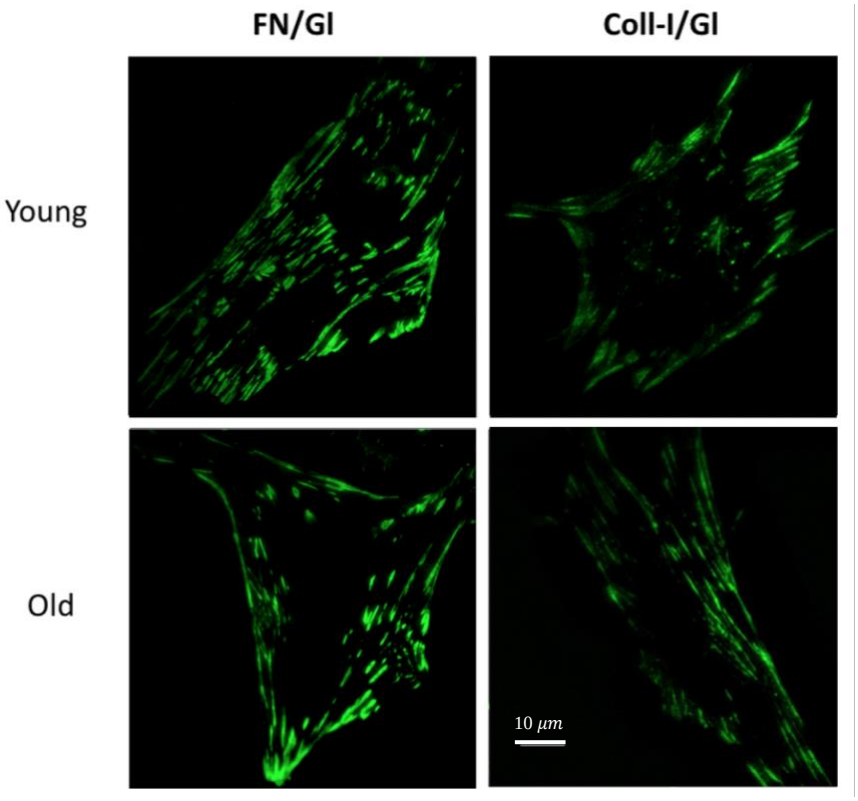

Figure 3.1: TIRF images of young and old VSMC plated on FN and Coll-1. The scale bar is 10 μm.

The higher fluorescence intensity observed in *young* cells, in **Figure 3.1**, indicates an increased β1 integrin recruitment at adhesions observed as streak-like fluorescent patches present throughout the cell area for VSMC plated on FN. In contrast, the reduced fluorescence intensity present at cell adhesions of *old* cells, indicates an age-induced reduction of integrin β1 localization at FA in aged VSMC. From a morphological point of view, aging causes a reduction of FA present at the basal cell level, mostly aligned along the outer edges of the cell. For cells plated on Coll-1, the same trend was recorded; however, the overall VSMC florescence is reduced, for young and old groups, in comparison with cells plated on FN.

The bar graphs presented in **Figure 3.2** show the quantitative values of the average integrin β1 protein ratio (i.e., protein area/cell area for each cell). A Student's t-test statistical analysis, was used to evaluate the results using a significance level of $P<0.05$, confirming a significant reduction of the average integrin β1 protein ratios between the young and old VSMC groups for FN and Coll-1. Thus, integrin β1 integrin recruitment was decreased in old VSMC plated on glass dishes functionalized with either matrix.

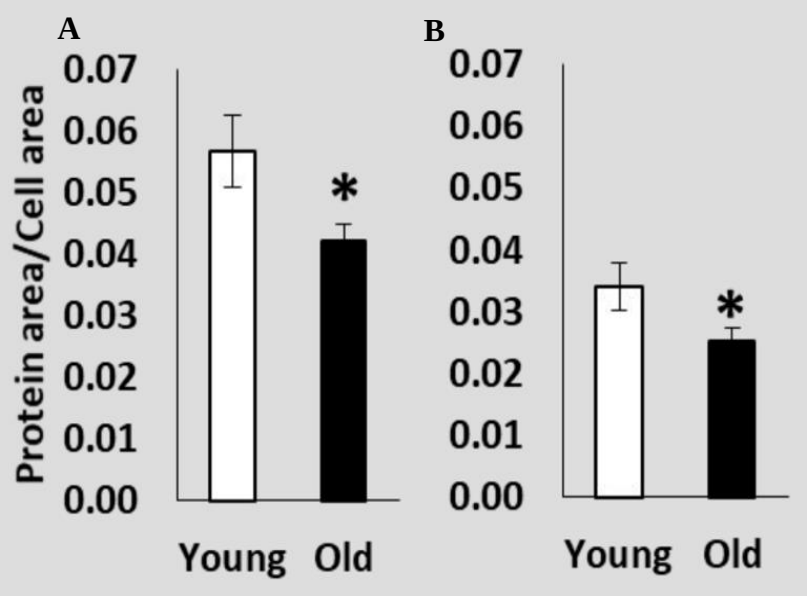

Figure 3.2: (A) Average protein ratio of integrin β1 in young and old VSMC plated on FN. (B) Average protein ratio of integrin β1 in young and old VSMC plated on Coll-1. Data shows mean ± SEM.

Figure 3.3 shows representative fluorescence images obtained using confocal microscopy. As previously mentioned, confocal microscopy records the protein fluorescence throughout the cell volume. In this figure, the difference in total fluorescence intensity between young and old VSMC can be observed for integrin β1 recruitment in both matrix proteins (FN and Coll-1) shown as streak-like patches.

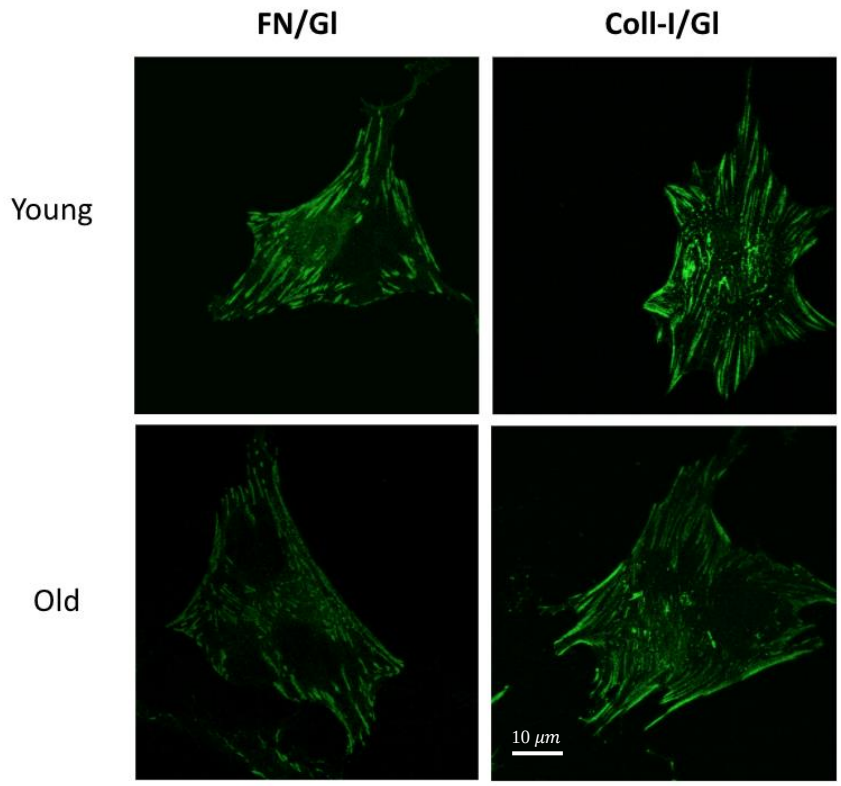

Figure 3.3: Confocal images of young and old VSMC plated on FN and Coll-1. The scale bar is 10 μm.

From **Figure 3.3**, a high fluorescence intensity is observed in *young* cells. Conversely, *old* cells display a reduced fluorescence intensity, which is concurrent with an age-induced reduction of integrin β1 expression for cells functionalized with both ECM proteins. Furthermore, old cells present more adhesions localized along cell edges.

The bar graph in **Figure 3.4** presents the quantitative results of the mean fluorescence intensity values of β1 integrin for young and old VSMC plated on glass bottom dishes functionalized with either FN or Coll-1.

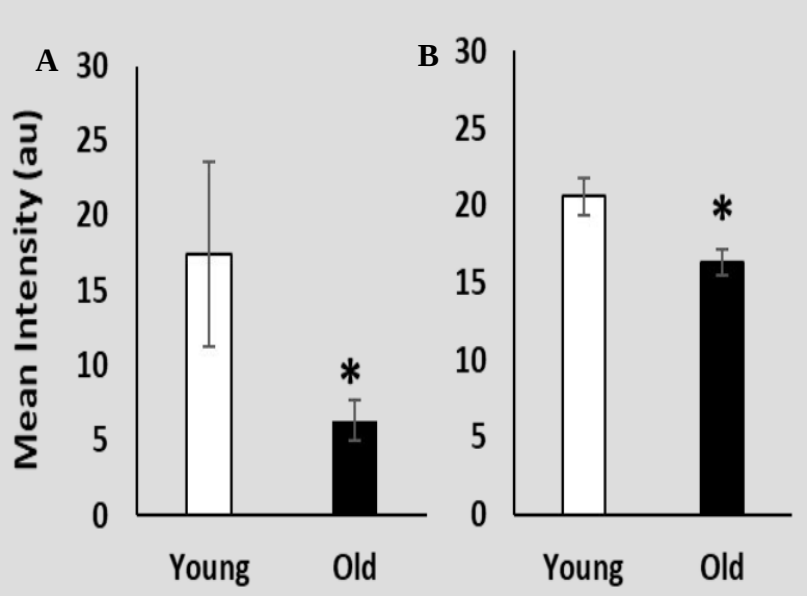

Figure 3.4: (A) Mean intensity in young and old VSMC plated on FN. (B) Mean intensity in young and old VSMC plated on Coll-1. Data shows mean ± SEM.

The intensity values from **Figure 3.4** represent the fluorescence observed throughout the entire VSMC volume. The morphological changes in old cells correspond to the significant difference of the mean integrin β1 intensity between the young and old VSMC groups for each matrix, as shown through statistical analysis using Student's t-test and considering a significance level of $P<0.05$.

4. CONCLUSION

Arterial aging represents a major contributor to CVDs present in older populations as it is characterized by reduced vessel contractility, arterial stiffening, and endothelial dysfunction. (Delp et al., 1995; Kenney & Armstrong, 1996; Dinenno et al., 2002; Qiu et al., 2010). In turn, the blood vessel's inability to properly regulate vessel tone can result in an impaired blood flow distribution and a reduced capacity for exercise in elderly (Davy et al., 1998; Musch et al., 2004). The correlation between aging and reduced arterial contractility has been associated with a phenotypic change in vascular smooth muscle cells, resulting in the decreased ability of cells to adapt to external stimuli.

This study is focused on analyzing the integrin role as a contributor to arterial vasomotor dysfunction through the regulation of vascular smooth muscle cells adhesion to extracellular matrix components. Specifically, this research focuses on measuring the $\beta 1$ integrin recruitment at FA for cells plated on glass dishes functionalized with Coll-I and FN. Using TIRF and confocal microscopy, $\beta 1$ protein expression in VSMC was quantified at sites of cell-matrix attachment and throughout the entire cell. The results showed a significantly lower fluorescence intensity in *old* cells, that corresponds to a decrease in integrin $\beta 1$ recruitment at FA in response to both ECM proteins. According to previous research, the significant decrease of integrin $\beta 1$ recruitment at cell-matrix adhesions in old cells indicates a reduced cell adhesion to the matrix, indicative of a decreased vessel contractility induced by aging.

REFERENCES

Alberts, B., Bray, D., Lewis, J., Raff, M., Roberts, K., & Watson, J. D. (1994). *Molecular Biology of the Cell. 3rd edition*. Garland Science.

Arnaout, M. A., Goodman, S. L., & Xiong, J. P. (2007). Structure and mechanics of integrin-based cell adhesion. *Curr Opin Cell Biol*, *19*(5), 495-507.

Davis, M. J., Wu, X., Nurkiewicz, T. R., Kawasaki, J., Davis, G. E., Hill, M. A., Meininger, G. A. (2001). Integrins and mechanotransduction of the vascular myogenic response, Am. J. Physiol. Heart Circ. Physiol. 280 (2001) H1427–1433.

Davy, K. P., Seals, D. R., and Tanaka, H. (1998). Augmented cardiopulmonary and integrative sympathetic baroreflexes but attenuated peripheral vasoconstriction with age. *Hypertension* 32, 298–304. doi: 10.1161/01.HYP.32.2.298

Delp, M. D., Brown, M., Laughlin, M. H., and Hasser, E. M. (1995). Rat aortic vasoreactivity is altered by old age and hindlimb unloading. *J. Appl. Physiol.* 78, 2079–2086. doi: 10.1152/jappl.1995.78.6.2079

Dinenno, F. A., Dietz, N. M., and Joyner, M. J. (2002). Aging and forearm postjunctional alpha-adrenergic vasoconstriction in healthy men. *Circulation* 106, 1349–1354. doi: 10.1161/01.CIR.0000028819.64790.BE

Donato, A. J., Machin, D. R., & Lesniewski, L. A. (2018). Mechanisms of Dysfunction in the Aging Vasculature and Role in Age-Related Disease. *Circulation research*, *123*(7), 825–848. https://doi.org/10.1161/CIRCRESAHA.118.312563

Geiger, B., Bershadsky, A., Pankov, R., & Yamada, K. M. (2001). Transmembrane crosstalk between the extracellular matrix--cytoskeleton crosstalk. *Nature reviews. Molecular cell biology*, *2*(11), 793–805. https://doi.org/10.1038/35099066

Hibbs, A. R. (2004). *Confocal microscopy for biologists*. Kluwer Academic/Plenum Publishers, New York.

Janmey, P. A., McCulloch, C. A. (2007). Cell mechanics: integrating cell responses to mechanical stimuli, Annu. Rev. Biomed. Eng. 9, 1–34.

Janmey, P. A., Winer, J. P., Murray, M. E., Wen, Q. (2009). The hard life of soft cells, Cell Motil. Cytoskeleton 66, 597–605.

Kenney, W. L., and Armstrong, C. G. (1996). Reflex peripheral vasoconstriction is diminished in older men. *J. Appl. Physiol.* 80, 512–515. doi: 10.1152/jappl.1996. 80.2.512

Lakatta, E. G. (2003). Arterial and cardiac aging: major shareholders in cardiovascular disease enterprises: part III: cellular and molecular clues to heart and arterial aging. *Circulation* 107, 490–497. doi: 10.1161/01.CIR.0000048894. 99865.02

Legate, K. R., & Fässler, R. (2009). Mechanisms that regulate adaptor binding to β-integrin cytoplasmic tails. *Journal of Cell Science, 122*(2), 187-198.

Lim, S. M., Kreipe, B. A., Trzeciakowski, J., Dangott, L., & Trache, A. (2010). Extracellular matrix effect on RhoA signaling modulation in vascular smooth muscle cells. *Experimental cell research*, *316*(17), 2833–2848. https://doi.org/10.1016/j.yexcr.2010.06.010

Luo, Y., Xu, X., Lele, T., Kumar, S., Ingber, D. E. (2008). A multi-modular tensegrity model of an actin stress fiber, J. Biomech. 41, 2379–2387.

Martin, K. H., Slack, J. K., Boerner, S. A., Martin, C. C., Parsons, J. T. (2002). Integrin connections map: to infinity and beyond, Science 296, 1652–1653.

Martinez-Lemus, L. A., Wu, X., Wilson, E., Hill, M. A., Davis, G.E., Davis, M. J., Meininger, G. A. (2003). Integrins as unique receptors for vascular control, J. Vasc. Res. 40. 211–233.

Morphic Therapeutic - *Integrin Biology* (2018). https://morphictx.com/our-technology/.

Musch, T. I., Eklund, K. E., Hageman, K. S., and Poole, D. C. (2004). Altered regional blood flow responses to submaximal exercise in older rats. *J. Appl. Physiol.* 96, 81–88. doi: 10.1152/japplphysiol.00729.2003

Najjar, S. S., Scuteri, A., & Lakatta, E. G. (2005). Arterial aging: is it an immutable cardiovascular risk factor? *Hypertension*, *46*(3), 454-462.

Ohja, K. R., Padgham S., Shin, S.Y., Leon Olmedo, F., Woodman, C. R. Trache, A. (2021). Substrate stiffness modulates integrin beta-1 recruitment at cell-matrix adhesions in aged vascular smooth muscle cells. 65th Biophysical Society Annual Meeting, February, 2021, Abstract 21-L-3472-BPS.

Opazo Saez, A., Zhang, W., Wu, Y., Turner, C. E., Tang, D. D., Gunst, S. J. (2004). Tension development during contractile stimulation of smooth muscle requires recruitment of paxillin and vinculin to the membrane, Am. J. Physiol. Cell Physiol. 286, C433–447.

Qiu, H., Zhu, Y., Sun, Z., Trzeciakowski, J. P., Gansner, M., Depre, C., et al. (2010). Short communication: vascular smooth muscle cell stiffness as a mechanism for increased aortic stiffness with aging. *Circ. Res.* 107, 615–619. doi: 10.1161/ CIRCRESAHA.110.221846

Saphirstein, R. J., Gao, Y. Z., Jensen, M. H., Gallant, C. M., Vetterkind, S., Moore, J. R., et al. (2013). The focal adhesion: a regulated component of aortic stiffness. *PLoS One* 8:e62461. doi: 10.1371/journal.pone.0062461

Seawright, J. W., Sreenivasappa, H., Gibbs, H. C., Padgham, S., Shin, S. Y., Chaponnier, C., Yeh, A. T., Trzeciakowski, J. P., Woodman, C. R., & Trache, A. (2018). Vascular Smooth Muscle Contractile Function Declines With Age in Skeletal Muscle Feed Arteries. *Frontiers in physiology*, *9*, 856. https://doi.org/10.3389/fphys.2018.00856

Takada, Y., Ye, X., & Simon, S. (2007). The integrins. *Genome biology*, *8*(5), 215. https://doi.org/10.1186/gb-2007-8-5-215

Trache, A., & Meininger, G. A. (2008). Total internal reflection fluorescence (TIRF) microscopy. *Current protocols in microbiology*, *Chapter 2*, . https://doi.org/10.1002/9780471729259.mc02a02s10

Trache, A., Massett, M.P., & Woodman, C. R. (2020). Vascular smooth muscle stiffness and its role in aging. *Membrane Biomechanics*, 217–253. https://doi.org/10.1016/bs.ctm.2020.08.008

Virani, S. S., Alonso, A., Aparicio, H. J., Benjamin, E. J., Bittencourt, M. S., Callaway, C. W., Carson, A. P., Chamberlain, A. M., Cheng, S., Delling, F. N., Elkind, M., Evenson, K. R., Ferguson, J. F., Gupta, D. K., Khan, S. S., Kissela, B. M., Knutson, K. L., Lee, C. D., Lewis, T. T., Liu, J., … (2021). American Heart Association Council on Epidemiology and Prevention Statistics Committee and Stroke Statistics Subcommittee. Heart Disease and Stroke Statistics-2021 Update: A Report From the American Heart Association. *Circulation*, *143*(8), e254–e743. https://doi.org/10.1161/CIR.0000000000000950

Virani, S. S., Alonso, A., Benjamin, E. J., Bittencourt, M. S., Callaway, C. W., Carson, A. P., Chamberlain, A. M., Chang, A. R., Cheng, S., Delling, F. N., Djousse, L., Elkind, M., Ferguson, J. F., Fornage, M., Khan, S. S., Kissela, B. M., Knutson, K. L., Kwan, T. W., Lackland, D. T., Lewis, T. T., … (2020). American Heart Association Council on Epidemiology and Prevention Statistics Committee and Stroke Statistics Subcommittee. Heart Disease and Stroke Statistics-2020 Update: A Report From the American Heart Association. *Circulation*, *141*(9), e139–e596. https://doi.org/10.1161/CIR.0000000000000757

Worth, N. F., Rolfe, B. E., Song, J., Campbell G. R., Vascular smooth muscle cell phenotypic modulation in culture is associated with reorganisation of contractile and cytoskeletal proteins, Cell Motil. (2001). Cytoskeleton 49, 130–145.

Yue B. (2014). Biology of the extracellular matrix: an overview. *Journal of glaucoma*, *23*(8 Suppl 1), S20–S23. https://doi.org/10.1097/IJG.0000000000000108

Zaidel-Bar, R., Itzkovitz, S., Ma'ayan, A., Iyengar, R., Geiger, B. (2007). Functional atlas of the integrin adhesome, Nat. Cell Biol. 9, 858–867.

Zamir, E., Geiger, B., (2001). Molecular complexity and dynamics of cell–matrix adhesions, J. Cell Sci. 114, 3583–3590.

Zhang, J., Zhao, X., Vatner, D. E., McNulty, T., Bishop, S., Sun, Z., et al. (2016). Extracellular matrix disarray as a mechanism for greater abdominal versus thoracic aortic stiffness with aging

in primates. *Arterioscler. Thromb. Vasc. Biol.* 36, 700–706. doi: 10.1161/ATVBAHA.115.306563